Nonlinear waves at the free surface of flexible mechanical metamaterials ⊘

Bolei Deng ⓘ ; Hang Shu ⓘ ; Jian Li ⓘ ; Chengyang Mo ⓘ ; Jordan R. Raney ⓘ ; Vincent Tournat ⓘ ;
Katia Bertoldi ✉ ⓘ

Check for updates

CrossMark

View
Online

Export
Citation

Articles You May Be Interested In

AIP
Publishing

Nonlinear waves at the free surface of flexible mechanical metamaterials

Bolei Deng,[1,2,3] (iD) Hang Shu,[4] (iD) Jian Li,[1,5] (iD) Chengyang Mo,[4] (iD) Jordan R. Raney,[4] (iD) Vincent Tournat,[1,6] (iD) and Katia Bertoldi[1,a)] (iD)

AFFILIATIONS

[1]Harvard John A. Paulson School of Engineering and Applied Sciences, Harvard University, Cambridge, Massachusetts 02138, USA
[2]Computer Science and Artificial Intelligence Laboratory, Massachusetts Institute of Technology, Cambridge, Massachusetts 02139, USA
[3]Department of Mechanical Engineering, Massachusetts Institute of Technology, Cambridge, Massachusetts 02139, USA
[4]Department of Mechanical Engineering and Applied Mechanics, University of Pennsylvania, Philadelphia, Pennsylvania 19104, USA
[5]Department of Engineering Mechanics, Zhejiang University, Hangzhou 310027, China
[6]Laboratoire d'Acoustique de l'Université du Mans (LAUM), UMR 6613, Institut d'Acoustique - Graduate School (IA-GS), CNRS, Le Mans Université, France

[a)]Author to whom correspondence should be addressed: bertoldi@seas.harvard.edu

ABSTRACT

In this Letter, we investigate the propagation of nonlinear pulses along the free surface of flexible metamaterials based on the rotating squares mechanism. While these metamaterials have previously been shown to support the propagation of elastic vector solitons through their bulk, here, we demonstrate that they can also support the stable propagation of nonlinear pulses along their free surface. Furthermore, we show that the stability of these surface pulses is higher when they minimally interact with the linear dispersive surface modes. Finally, we provide guidelines to select geometries that minimize these interactions.

Published under an exclusive license by AIP Publishing. https://doi.org/10.1063/5.0135375

Surface waves that propagate along the boundary of a medium play a key role in a variety of natural and man-made systems. Seismic surface waves cause the ground to shake,[1] and surface gravity waves can be observed on rivers, lakes, and oceans.[2] Furthermore, surface ultrasonic waves are harnessed in nondestructive testing to detect cracks or corrosion,[3,4] and surface acoustic waves are commonly used to realize electronic systems.[5,6] It is, therefore, important to investigate the physics of surface waves in order to advance technology.

Ongoing advances in fabrication are enabling the realization of mechanical metamaterials capable of manipulating elastic waves in unprecedented ways. These have been used to enable the design of waveguides and filters,[7] energy absorbers,[8] energy harvesters,[9] and vibration isolators.[10] They have also provided a powerful platform to investigate and observe surface waves[11,12] and topologically protected edge modes.[13–17] While most mechanical metamaterials operate in the linear regime, it has been recently shown that large deformations and instabilities can be exploited to manipulate the propagation of finite amplitude elastic waves.[18–30] However, to date, most studies have focused on nonlinear pulses propagating in the bulk of these flexible metamaterials. The propagation of large amplitude pulses on their free surfaces has received little attention.

In this Letter, we combine experiments and simulations to investigate the propagation of nonlinear waves on the free surface of a flexible metamaterial comprising a network of squares connected by thin and highly deformable ligaments. Recent studies that focus on the propagation of vector solitons through the bulk of such metamaterials have hinted at the existence of large amplitude pulses with stable shape localized at their free surfaces[25] [Fig. 1(a)]. Motivated by these observations, we systematically investigate the propagation of large amplitude waves on the surface of a rectangular sample. We find that the system supports surface pulses with coupled displacements and rotations that retain their shape during propagation. Furthermore, we numerically investigate the stability of these surface pulses and find that the less they interact with the excited linear surface dispersive modes, the more stable they are.

We consider a 32×24 array of squares fabricated out of polydimethylsiloxane (PDMS) with a thickness of 8 mm using direct ink writing.[23,25,31] The squares are rotated by offset angles of $\theta_0 = 25°$
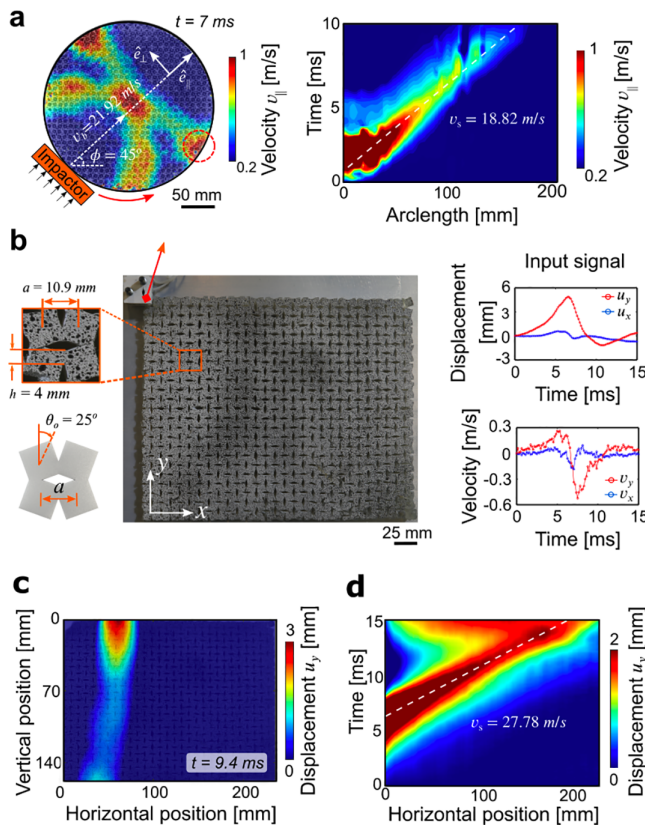
FIG. 1. (a) Experimental snapshot at $t = 7$ ms of a 2D circular sample with 30 squares along its diameter when excited with an impactor at 45° angle [Reprinted with permission from Deng *et al.*,[25] Phys. Rev. Lett. **123**, 024101 (2019). Copyright 2019 American Physical Society]. The color represents the velocity along the direction of the impact ($v_\parallel$). The impact also excites a large amplitude pulse that propagates along the free surface with nearly constant velocity (see red dashed circle in the snapshot and spatiotemporal plot of $v_\parallel$ along the surface). (b) Snapshot of the system tested for this study (left). Excitation profile of the impacted unit cell (right). (c) Contour plot of the vertical displacement (u_y) at time $t = 9.4$ ms after impact. (d) Spatiotemporal map of u_y along the top surface.

with a center-to-center-distance of $a = 10.89$ mm and are connected to one another by flexible ligaments with widths of approximately 4 mm [Fig. 1(b)]. In our experiments, we use a customized polylactide (PLA) impactor to apply an impulse to the top left corner of the sample [Fig. 1(b)]. To characterize the propagation of the excited pulses, we record the experiments with a high-speed camera (Photron FASTCAM Mini AX) and extract the displacement and velocity of each square unit.

Figure 1(c) shows the contour plot of the vertical displacement (u_y) at $t = 9.4$ ms after impact. The impact excites a pulse with the energy mostly localized close to the top surface. To further characterize the propagation of this pulse, we generate the spatiotemporal map of u_y along the top row of the sample [Fig. 1(d)]. This indicates that a single pulse is formed and propagates at a speed of $c \simeq 28$ m/s until it reaches the end of the specimen.

Next, we make use of numerical simulations to systematically explore the characteristics of the nonlinear pulses that propagate along

the surface of the metamaterial. We model the system as an array of rigid squares, each with mass $m = 0.4$ g and moment of inertia $J = 4.8$ g mm². Each square has three degrees of freedom (displacements u_x and u_y and rotation θ) and is connected to the neighbors via a combination of linear longitudinal (with experimentally measured stiffness $k_l = 19237$ N/m), shear ($k_s = 9618$ N/m), and rotational springs ($k_\theta = 0.0507$ N m/rad).[25] By imposing force equilibrium at each unit, we derive a system of coupled nonlinear ordinary differential equations that we numerically integrate to obtain the response of the structure.[26] In our simulations, we consider a larger system comprising 50×25 squares to minimize boundary effects, apply the experimentally extracted displacement signal shown in Fig. 1(b) to four squares on the top left corner [highlighted in red in Fig. 2(a)], and implement free-boundary conditions everywhere else. Finally, to prevent reflections from the bottom surface, we add progressively increasing damping to the bottom ten rows of the model.

In Fig. 2(a), we report the numerically predicted contour plot of u_y at time $t = 12.8$ ms after the impact. We find that the applied input excites a pulse with a width of $\simeq 5$ squares that remains mostly localized on the top surface. This suggests that dispersion should occur, since the wavelength of the wave is comparable to the spatial period of the structure. In order to analyze the stability of such large amplitude pulses during propagation, in Fig. 2(b), we report the spatial-temporal map of u_y along the top row of the sample. Furthermore, in Fig. 2(c), we show the evolution of the vertical (u_y) and horizontal (u_x) displacement components of the pulse as a function of space along the top surface at $t = 6, 11.2$, and 16.3 ms. (Note that in our 2D system, these surface nonlinear waves are effectively edge waves.) While the former indicates that the pulse travels along the surface with a relatively constant velocity and width, the latter shows that its amplitude and shape vary during propagation. Since such variation could be due to an applied impact that results in a displacement signal far from that of a potentially supported solitary wave, we then use the numerical signal collected at the 25th unit [which we fit with derivatives of Gaussian functions—Fig. 2(d)] as new impact signals for both the u_x and u_y components. As shown in Fig. 2(e), this input initially results in a more stable propagation along the surface, closer to what one would expect from a solitary wave. However, when simulating a longer sample comprising 200×25 units, we find that the pulse gets largely distorted after a propagation distance of ≈ 100 units [Fig. 2(f)]—likely because of interactions with the linear surface waves. To better quantify this distortion, we introduce the ratio

$$\eta(t) = \frac{\sum\limits_{i \in Set_p} \left[u_y^{[1,i]}(t) \right]^2}{\sum\limits_{i=1}^{200} \left[u_y^{[1,i]}(t) \right]^2}, \tag{1}$$

where $u_y^{[1,i]}(t)$ is the displacement of the i-th square on the top surface along the y-direction at time t and Set_p denotes the set of squares on the top surface that are in the nonlinear pulse. This set comprises the squares for which $x^{[1,i]} \in [x_0 - 3W, x_0 + 3W]$, where x_0 and W denote the position and width of the nonlinear pulse, respectively, which are identified by fitting $u_y^{[1,i]}$ with a bell-shape curve ($A \mathrm{sech}((x - x_0)/W)$). As shown in Fig. 2(f), we find that η is close to 1 at $t = 20$ ms, confirming that the energy is initially concentrated in the nonlinear pulse. However, during propagation, η monotonically
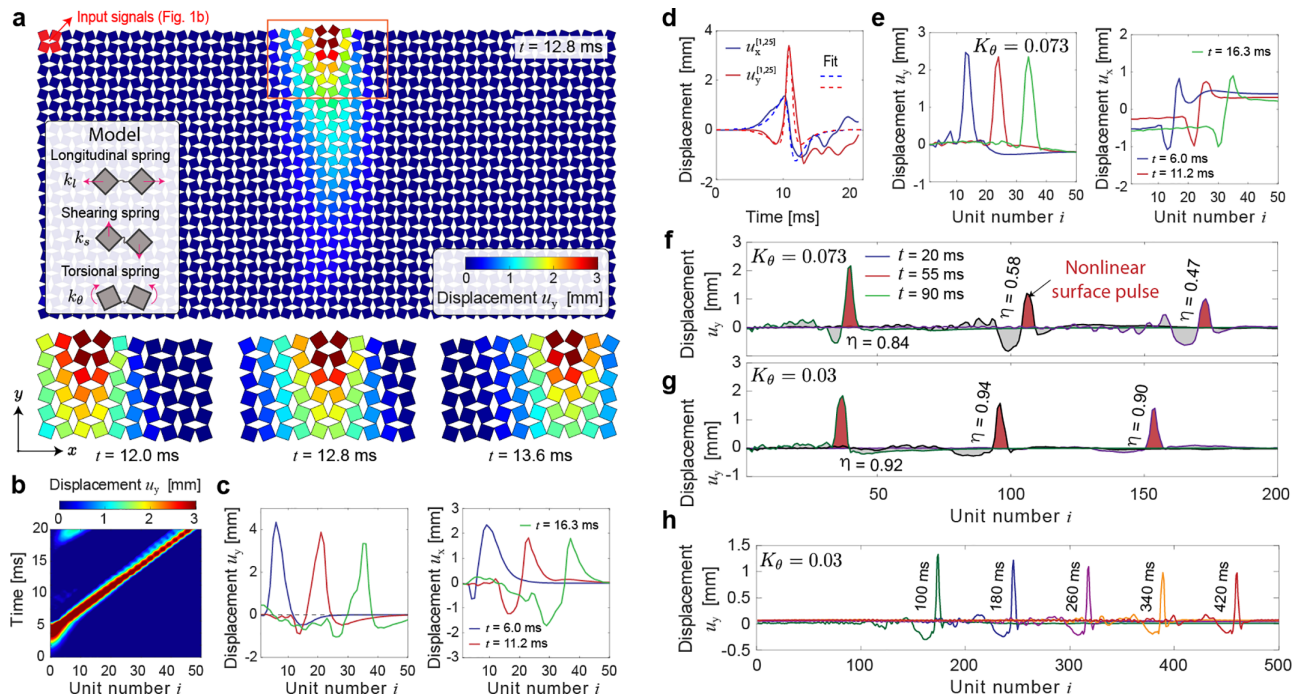
FIG. 2. (a)–(e) Numerical results for a model comprising 50×25 squares. (a) Contour plots of u_y over the entire model at $t = 12.8$ ms after impact and in a region close to the top surface at $t = 12.0$, 12.8, and 13.6 ms. The pulse is excited by applying the experimentally extracted displacement signal shown in Fig. 1(b) to the four squares highlighted in red. (b) Spatiotemporal map of u_y along the top surface. (c) Spatial displacement profiles along the top surface at $t = 6.0$, 11.2, and 16.3 ms. (d) The signal collected at the 25th unit (continuous lines) is fitted with derivatives of Gaussian functions (dashed lines). (e) Spatial displacement profiles along the top surface at $t = 6.0$, 11.2, and 16.3 ms when the model is excited by applying the signal shown in (b). (f)–(g) Numerical results for a model comprising 200×50 squares. Spatial displacement profiles along the top surface at $t = 20.0$, 55.0, and 90.0 ms with (f) $K_\theta = 0.073$ and (g) $K_\theta = 0.03$ when excited by applying the signal shown in (d). (h) Numerical results for a long sample comprising 500×50 squares. Spatial displacement u_y profiles along the top surface at $t = 100$, 180, 260, 340, and 420 ms when excited by applying the signal shown in (d).

decreases ($\eta = 0.58$ and 0.47 at $t = 55$ and 90 ms, respectively), indicating that the energy progressively leaks out of the nonlinear pulse.

Interestingly, our simulations also indicate that the distortion of the pulse is largely affected by the mechanical properties of the hinges. By changing the torsional stiffness from $K_\theta = 4k_\theta \cos^2\theta_0/(k_l a^2)$ $= 0.073$ [Fig. 2(f)] to $K_\theta = 0.03$ [Fig. 2(g)], we obtain a surface pulse that seems to be able to propagate stably with nearly constant shape, amplitude, and speed over 200 units. In this case, we find that $\eta \approx 0.9$ during the entire propagation. Note that additional simulations show that the pulse maintains its shape and velocity even when propagating over 500 units [Fig. 2(h)], providing further evidence for the existence of surface solitary waves in our system.

To verify our hypothesis that the distortion of the nonlinear pulses is caused by interactions with linear surface modes, we calculate the band structure of the system. To this end, we perform one-dimensional Bloch wave analysis on a supercell comprising 25×2 square units, assuming free-boundary conditions for the top and bottom edges. As reported in Fig. 3(c) for a structure characterized by $K_\theta = 0.03$, the band structure shows both bulk modes with motion distributed over the entire supercell (see modes *iii–vi*) and surface modes localized at the free boundary (see modes *i* and *ii*). Such surface modes occur at lower frequencies than the bulk modes for comparable wavelengths and are dispersive. Next, we compare these linear modes to the dispersion curves extracted from the nonlinear pulses reported

in Figs. 2(f) and 2(g) via a double Fourier transform (from space-time to wave number-frequency). We find that the dispersion curves of the linear and nonlinear surface waves are very close to each other for the metamaterials with both $K_\theta = 0.03$ [Fig. 3(b)] and $K_\theta = 0.073$ [Fig. 3(c)]. However, the nonlinear surface pulses are characterized by a non-dispersive propagation (i.e., they are a straight line) unlike the dispersion predicted for linear surface modes. This indicates that for the nonlinear pulses, the linear dispersion is compensated by either nonlinear distortion effects[23,24] or nonlinear dispersion effects.[32–34]

In order to quantify the proximity between the linear surface modes and the nonlinear surface pulses, in Figs. 3(d) and 3(e), we report the group velocities as a function of the wavenumber of the linear (green lines) and nonlinear (red lines) pulses for $K_\theta = 0.03$ and 0.073. As expected, we find that the group velocity is constant for the nonlinear modes (i.e., $v_g/v_0 \approx 0.38$ for $K_\theta = 0.03$ and $v_g/v_0 \approx 0.41$ for $K_\theta = 0.073$), whereas it varies as a function of the wave number for the linear ones. Furthermore, it appears that for the metamaterial with $K_\theta = 0.03$, the group velocity of the nonlinear pulse is, for most wavenumbers, larger than the one of linear modes [Fig. 3(d)], ensuring separation and weak interactions between them. By contrast, for the structure with $K_\theta = 0.073$, the group velocity of the linear waves is larger than that of the nonlinear pulse over a wider range of wavenumbers [see area highlighted in red in Fig. 3(e)]. It follows that, in this case, the linear waves propagate faster than the nonlinear pulse for a
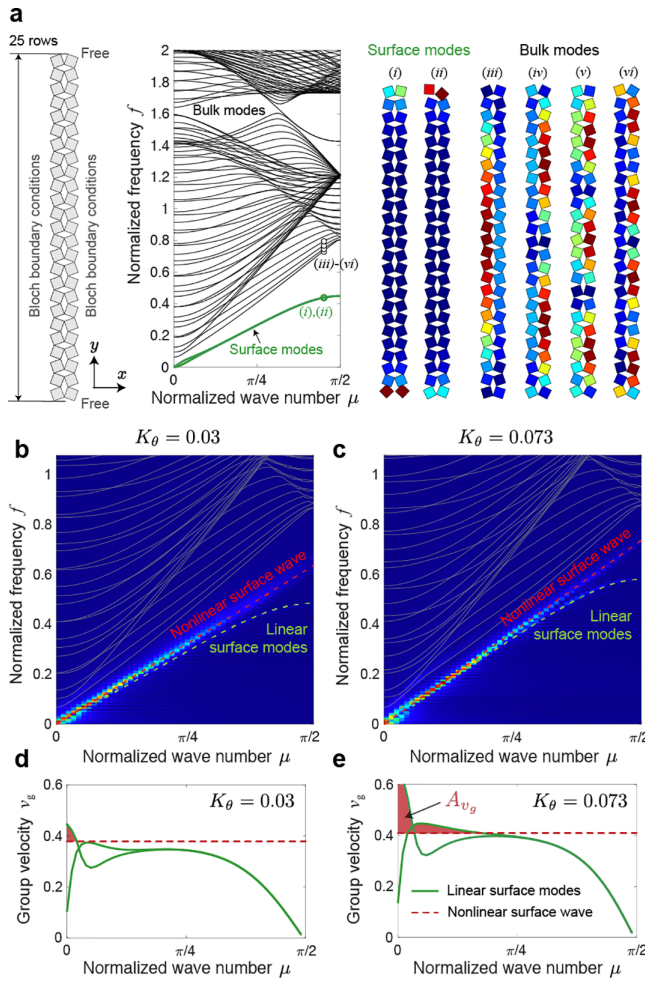
FIG. 3. (a) 1D band structure showing bulk bands (black lines) and edge bands (green lines). Modal deformation fields of surfaces (i)–(ii) and bulk (iii)–(vi) modes. The colors indicate the rotation of each unit (with dark blue corresponding to no rotation and dark red to maximum rotation). (b) and (c) Comparison between the linear modes and the dispersion curves extracted from the nonlinear pulses reported in Figs. 2(f) and 2(g) via a double Fourier transform (from space-time to wave number-frequency) for (b) $K_\theta = 0.03$ and (c) $K_\theta = 0.073$. (d)–(e) Group velocity of the nonlinear (red lines) and linear (green lines) surface waves for (d) $K_\theta = 0.03$ and (e) $K_\theta = 0.73$.
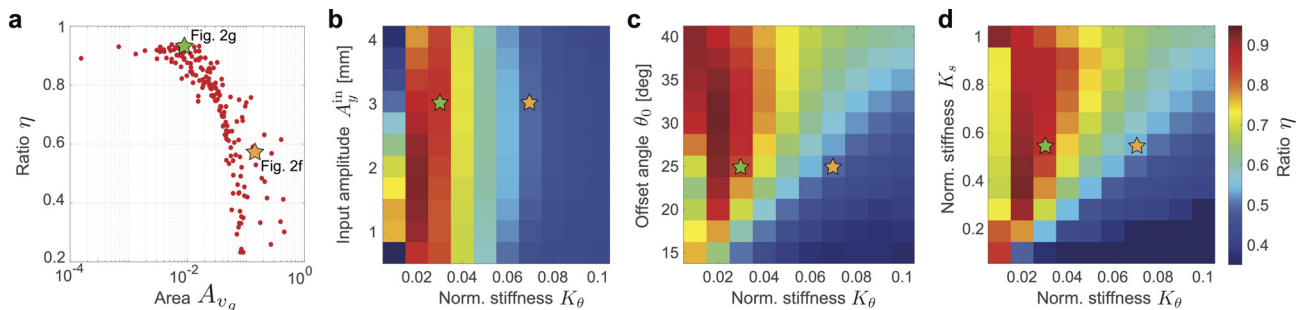
wide range of wavenumbers, and this promotes interactions between them that ultimately lead to distortion of the nonlinear pulse during propagation. To quantify such interactions, we calculate the area A_{v_g} of the region below v_g of the linear surface modes, but above that of the nonlinear pulse [see regions highlighted in red in Figs. 3(d) and 3(e)]. For the two structures with $K_\theta = 0.073$ and $K_\theta = 0.03$, we find that $A_{v_g} = 0.15$ and 0.009, respectively.

Finally, to confirm the connection between the distortion of the nonlinear pulses and proximity between the linear and nonlinear surface modes, we simulate 330 systems characterized by $K_\theta \in [0.01, 0.1]$, $K_s = k_s/k_l \in [0.1, 1]$, and $\theta_0 \in [15°, 40°]$ and input amplitude $A \in [1\,\text{mm}, 4\,\text{mm}]$. From each simulation, we extract the mean value of η [defined in Eq. (1) and averaged over ten values calculated at ten times between 55 and 90 ms] as well as A_{v_g}. As shown in Fig. 4(a), we find that the smaller is A_{v_g} (i.e., the more separation is between the group velocities of the linear and nonlinear surface pulses) and the higher is η (i.e., the more energy is concentrated in the nonlinear pulses). This observation clearly confirms that, for a given metamaterial design, nonlinear pulses are more stable when they weakly interact with the linear modes—a condition that is achieved when the group velocity of the nonlinear waves is greater than that of linear modes over a wide wavenumber range. Furthermore, our results indicate that the ratio η strongly depends on the geometric parameters of the metamaterial. Stable propagation (i.e., $\eta \to 1$) is found for $K_\theta \simeq 0.02$ [Figs. 4(b)–4(d)], input amplitude $A^{in} \simeq 2$ mm [Fig. 4(b)], offset angle $\theta_0 \simeq 30°$ [Fig. 4(c)], and dimensionless shear stiffness $K_s = k_s/k_l \simeq 0.5$ [Fig. 4(d)]. As such, these results provide guidelines to identify flexible metamaterials based on the rotating squares mechanism that can support stable propagation of large amplitude pulses on their free surfaces.

To summarize, we have demonstrated that flexible metamaterials based on the rotating squares mechanism can support the propagation of solitary-like nonlinear wave pulses along their free surfaces. Our results indicate that the nonlinear pulses can propagate for a significant distance along the surface retaining their shape when their interactions with the linear surface dispersive modes are minimal. In practice, this condition is realized when the nonlinear pulses possess a larger group velocity than the linear surface modes for most wavenumbers. The observed nonlinear surface waves in our system demonstrate certain similarities with topologically protected edge modes,[35] which might be considered a nonlinear version or extension of these linear phenomena. However, further research is needed to investigate

FIG. 4. (a) Relation between η and A_{v_g} for the 330 simulated metamaterials. (b)–(d) Evolution of η as a function of K_θ, K_s, input amplitude A_{in}, and offset angle θ_0. The green and yellow stars correspond to the two structures considered in Figs. 2(f) and 2(g), respectively.

the robustness of these waves at uneven surfaces and corners. Although our numerical simulations offer ample evidence of the existence of nonlinear surface pulses, we have not yet been able to derive analytical solutions to prove their solitary nature—a challenge for future work. Finally, we want to highlight the remarkable potential offered by the ability to control the interactions between linear and nonlinear waves on the surface of mechanical metamaterials. This capability opens up new avenues for manipulating seismic waves as well as for the design of filters that selectively block the propagation of certain nonlinear waves based on their group velocities and waveguides that allow for the propagation of nonlinear waves without distortion or attenuation. These applications exemplify the profound implications that arise from understanding and controlling the interactions between linear and nonlinear waves in flexible metamaterials.

AUTHOR DECLARATIONS
Conflict of Interest

The authors have no conflicts to disclose.

Author Contributions

Bolei Deng: Conceptualization (equal); Formal analysis (equal); Investigation (equal); Methodology (equal); Software (equal); Visualization (equal); Writing – original draft (equal); Writing – review & editing (equal). **Hang Shu:** Formal analysis (equal); Investigation (equal); Methodology (equal); Software (supporting); Visualization (equal); Writing – original draft (supporting); Writing – review & editing (supporting). **Jian Li:** Formal analysis (equal); Investigation (supporting); Software (equal). **Chengyang Mo:** Methodology (equal). **Jordan R. Raney:** Conceptualization (equal); Funding acquisition (equal); Methodology (equal); Resources (equal); Supervision (equal); Writing – review & editing (supporting). **Vincent Tournat:** Conceptualization (equal); Funding acquisition (equal); Investigation (supporting); Methodology (equal); Supervision (equal); Writing – original draft (equal); Writing – review & editing (equal). **Katia Bertoldi:** Conceptualization (equal); Funding acquisition (equal); Methodology (equal); Resources (equal); Supervision (equal); Writing – review & editing (equal).

DATA AVAILABILITY

The data that support the findings of this study are available from the corresponding author upon reasonable request.

REFERENCES

[1] A. Ben-Menahem and S. J. Singh, *Seismic Waves and Sources* (Springer Science & Business Media, 2012).

[2] B. Méhauté, *An Introduction to Hydrodynamics and Water Waves* (Springer, Berlin Heidelberg, 1976).

[3] D. Dhital and J.-R. Lee, "A fully non-contact ultrasonic propagation imaging system for closed surface crack evaluation," Exp. Mech. **52**, 1111–1122 (2012).

[4] S. K. Dwivedi, M. Vishwakarma, and A. Soni, "Advances and researches on nondestructive testing: A review," Mater. Today: Proc. **5**, 3690–3698 (2018).

[5] D. Morgan, *Surface Acoustic Wave Filters: With Applications to Electronic Communications and Signal Processing* (Academic Press, 2010).

[6] K. Länge, B. E. Rapp, and M. Rapp, "Surface acoustic wave biosensors: A review," Anal. Bioanal. Chem. **391**, 1509–1519 (2008).

[7] P. A. Deymier, *Acoustic Metamaterials and Phononic Crystals* (Springer, London, 2013).

[8] T. Frenzel, C. Findeisen, M. Kadic, P. Gumbsch, and M. Wegener, "Tailored buckling microlattices as reusable light-weight shock absorbers," Adv. Mater. **28**, 5865–5870 (2016).

[9] M. Carrara, M. R. Cacan, J. Toussaint, M. J. Leamy, M. Ruzzene, and A. Erturk, "Metamaterial-inspired structures and concepts for elastoacoustic wave energy harvesting," Smart Mater. Struct. **22**, 065004 (2013).

[10] J. Mei, G. Ma, M. Yang, Z. Yang, W. Wen, and P. Sheng, "Dark acoustic metamaterials as super absorbers for low-frequency sound," Nat. Commun. **3**, 756 (2012).

[11] S. Brûlé, E. Javelaud, S. Enoch, and S. Guenneau, "Experiments on seismic metamaterials: Molding surface waves," Phys. Rev. Lett. **112**, 133901 (2014).

[12] D. Mu, H. Shu, L. Zhao, and S. An, "A review of research on seismic metamaterials," Adv. Eng. Mater. **22**, 1901148 (2020).

[13] M. Miniaci, R. Pal, B. Morvan, and M. Ruzzene, "Experimental observation of topologically protected helical edge modes in patterned elastic plates," Phys. Rev. X **8**, 031074 (2018).

[14] X. Ni, C. He, X.-C. Sun, X.-P. Liu, M.-H. Lu, L. Feng, and Y.-F. Chen, "Topologically protected one-way edge mode in networks of acoustic resonators with circulating air flow," New J. Phys. **17**, 053016 (2015).

[15] S. D. Huber, "Topological mechanics," Nat. Phys. **12**, 621–623 (2016).

[16] M. Serra-Garcia, V. Peri, R. Süsstrunk, O. R. Bilal, T. Larsen, L. G. Villanueva, and S. D. Huber, "Observation of a phononic quadrupole topological insulator," Nature **555**, 342–345 (2018).

[17] H. Fan, B. Xia, L. Tong, S. Zheng, and D. Yu, "Elastic higher-order topological insulator with topologically protected corner states," Phys. Rev. Lett. **122**, 204301 (2019).

[18] F. Fraternali, G. Carpentieri, A. Amendola, R. E. Skelton, and V. F. Nesterenko, "Multiscale tunability of solitary wave dynamics in tensegrity metamaterials," Appl. Phys. Lett. **105**, 201903 (2014).

[19] J. R. Raney, N. Nadkarni, C. Daraio, D. M. Kochmann, J. A. Lewis, and K. Bertoldi, "Stable propagation of mechanical signals in soft media using stored elastic energy," Proc. Natl. Acad. Sci. U. S. A. **113**, 9722–9727 (2016).

[20] M. Hwang and A. F. Arrieta, "Solitary waves in bistable lattices with stiffness grading: Augmenting propagation control," Phys. Rev. E **98**, 042205 (2018).

[21] H. Yasuda, Y. Miyazawa, E. G. Charalampidis, C. Chong, P. G. Kevrekidis, and J. Yang, "Origami-based impact mitigation via rarefaction solitary wave creation," Sci. Adv. **5**, eaau2835 (2019).

[22] B. Deng, J. R. Raney, K. Bertoldi, and V. Tournat, "Nonlinear waves in flexible mechanical metamaterials," J. Appl. Phys. **130**, 040901 (2021).

[23] B. Deng, J. Raney, V. Tournat, and K. Bertoldi, "Elastic vector solitons in soft architected materials," Phys. Rev. Lett. **118**, 204102 (2017).

[24] B. Deng, P. Wang, Q. He, V. Tournat, and K. Bertoldi, "Metamaterials with amplitude gaps for elastic solitons," Nat. Commun. **9**, 3410 (2018).

[25] B. Deng, C. Mo, V. Tournat, K. Bertoldi, and J. R. Raney, "Focusing and mode separation of elastic vector solitons in a 2D soft mechanical metamaterial," Phys. Rev. Lett. **123**, 024101 (2019).

[26] B. Deng, V. Tournat, and K. Bertoldi, "Effect of predeformation on the propagation of vector solitons in flexible mechanical metamaterials," Phys. Rev. E **98**, 053001 (2018).

[27] H. Yasuda, L. M. Korpas, and J. R. Raney, "Transition waves and formation of domain walls in multistable mechanical metamaterials," Phys. Rev. Appl. **13**, 054067 (2020).

[28]J. Li, Y. Yuan, J. Wang, R. Bao, and W. Chen, "Propagation of nonlinear waves in graded flexible metamaterials," Int. J. Impact Eng. **156**, 103924 (2021).

[29]K. Pajunen, P. Johanns, R. K. Pal, J. J. Rimoli, and C. Daraio, "Design and impact response of 3D-printable tensegrity-inspired structures," Mater. Des. **182**, 107966 (2019).

[30]S. Qaderi, M. Ghadiri, M. Najafi, A. Imam, and H. Soleimanimehr, "Size-dependent nonlinear vibration analysis of cracked graphene-platelets-reinforced-composites (GPLRC) plate under parametric excitation," Commun. Nonlinear Sci. Numer. Simul. **121**, 107232 (2023).

[31]J. A. Lewis, "Direct ink writing of 3D functional materials," Adv. Funct. Mater. **16**, 2193–2204 (2006).

[32]V. F. Nesterenko, "Waves in strongly nonlinear discrete systems," Philos. Trans. R. Soc. A: Math., Phys. Eng. Sci. **376**, 20170130 (2018).

[33]P. Rosenau and J. M. Hyman, "Compactons: Solitons with finite wavelength," Phys. Rev. Lett. **70**, 564–567 (1993).

[34]P. Rosenau and A. Zilburg, "Compactons," J. Phys. A: Math. Theor. **51**, 343001 (2018).

[35]O. R. Bilal, R. Süsstrunk, C. Daraio, and S. D. Huber, "Intrinsically polar elastic metamaterials," Adv. Mater. **29**, 1700540 (2017).

02 October 2023 12:32:45